Self-consistent electronic structure of 7- and 19-layer Cu(001) films

Armando Euceda, D. M. Bylander, Leonard Kleinman, and Kenneth Mednick*
Department of Physics, The University of Texas, Austin, Texas 78712
(Received 8 February 1982)

Employing the self-consistent linear combination of Gaussian-orbital method, the energy bands of 7- and 19-layer Cu(001) films are calculated with greater numerical accuracy than previously used in the pioneering calculation of Smith *et al.* This leads to somewhat different surface-charge-density contours and calculated work functions but the large number of *d*-band surface states that they obtained are essentially reproduced here. A new iterative procedure is described which makes the convergence 2–3 times more rapid than standard methods.

I. INTRODUCTION

Our early parametrized (001), (110), and (111) Cu thin-film calculations[1] produced Shockley surface-state bands in most of the energy gaps throughout the two-dimensional Brillouin zone (2D BZ). Similar calculations[2] for Ni produced not only the Shockley bands but also Tamm surface-state bands lying above the top of the Ni *d* bands. These Tamm bands, which have since been confirmed by angle-resolved photoemission data,[3] are due to the narrowing of the surface *d* density of states (DOS) which causes an excess surface electronic charge which in turn causes a repulsive surface Coulomb potential which both reduces the excess surface charge and pushes the Tamm surface bands out of the top of the *d* bands. Because the *d* bands lie well below the Fermi energy, the same effect does not occur in Cu. Thus it came as a surprise when the self-consistent Cu(001) thin-film calculation of Smith, Gay, and Arlinghaus[4] (SGA) yielded Tamm bands even more strongly pushed out of the top of the *d* bands than those in Ni. These surface bands have also been observed with photoemission[5] both for (001) and (111) Cu but to add to the puzzle they were not found in the self-consistent Cu(111) calculation of Appelbaum and Hamann.[6]

This is the first of two papers in which we calculate the surface electronic structure of (001) and (111) Cu, using greater numerical accuracy than that of the pioneering calculations.[4,6] In the next section we compare our computational methods with those of SGA and in Sec. III present our results for 7- and 19-layer Cu(001) films. In Sec. IV we briefly discuss the results and give a physical argument to explain why the Tamm states are stronger in Cu than in Ni. In the Appendix we describe a new procedure for averaging old input and output potentials to obtain the next input potential on the path to self-consistency. This process converges 2 or 3 times more rapidly than standard methods and thus compensates for the greater amount of computer time required per iteration for these more numerically accurate calculations.

II. COMPUTATIONAL METHODS

Our basis set consists of 1*s*, 2*s*, 2*p*, 3*s*, 3*d*, 4*s*, and 4*p* atomic-orbital planar Bloch functions (expanded in Gaussians for computational ease) plus single Gaussian *s*, *p*, and *d* planar Bloch functions, $e^{-\alpha r^2}$, with $\alpha=0.1$ (for *s* and *p*) and $\alpha=0.13$ bohr^{-2} (for *d*), plus a second set with $\alpha=0.25$ bohr^{-2} (*s* and *p*) and $\alpha=0.4$ bohr^{-2} (for *d*) on the surface planes only, plus a set of $\alpha=0.3$ bohr^{-2} *s* and *p* planar Bloch functions floating in the empty sites 0.3 interplanar spacings above the surface planes. This set differs from that used by SGA in that they had no 4*p* atomic orbital (they did use a single diffuse *p* Gaussian) and they did not have a second set of surface-plane Gaussians nor the floating-plane Gaussians. In this calculation we found a projected charge density of 0.79 *p* electrons per atom and 0.33 *s* electrons per atom for the interior planes; thus it is desirable to have as much variational freedom for the *p* electrons as for the *s*. The extra surface variational freedom and especially the floating Gaussians are required for high accuracy in the surface-charge distribution and work function.[7] A comparison of our contour plot (Fig. 2) with that of SGA shows that our outermost contours are significantly flatter.

Both we and SGA used the same 15-point sample of the $\frac{1}{8}$th irreducible 2D BZ consisting of five $\bar{\Sigma}$ points and ten $\bar{k}$ points of no symmetry (see their Fig. 5). This sample which corresponds to 100 points in the full 2D BZ should be superior to the other possible 15-point sample consisting of $\bar{\Gamma},\bar{X},\bar{M}$ and three each of $\bar{\Sigma},\bar{\Delta},\bar{Y}$, and three general $\bar{k}$ points

which corresponds to a 64-point sample of the full 2D BZ. Both calculations were made with identical Hamiltonians containing Kohn-Sham exchange and Wigner correlation potentials so that any differences between the two must be due to computational errors, differences in the basis sets, or, most likely, the different methods used to fit the charge density and potential after each iteration.

SGA calculated the charge density and exchange-correlation potential on a regular mesh of 763 points in the $\frac{1}{16}$th irreducible wedge of the unit cell of their 9-layer film. We used 3200 points in our 7-layer (10-layer including selvage region) irreducible wedge. Of these, 644 (161 per atom) are on radial meshes at random angles about each atom, and the rest were chosen randomly throughout the wedge. It has been our experience that a smaller rms error in the charge-density fit is obtained when a regular mesh is used but that the fit tends to have large oscillations between the points which do not occur when the fit is made at randomly selected points. SGA assumed that the thin-film charge density differs from that of superposition of atoms only in its long-wavelength Fourier components and thus Fourier transformed the difference between their initial and latest charge density and exchange-correlation potential at each iteration. Because their atomic configuration is $3d^{10}4s^{1}$ whereas the crystal configuration is approximately $3d^{9.89}4s^{0.33},4p^{0.79}$, it seems to us that the short-wavelength Fourier components cannot be completely negligible. Halving their sampling mesh size (for a 5-layer film), and therefore increasing the number of Fourier components calculated by a factor of 8, SGA found a negligible change in their total density of states. Although they did not report it, Smith has informed us that the work function of SGA was unchanged to two decimal places and that their failure to achieve charge neutrality with their fit was reduced by a factor of 20 with the better sample. These results were obtained only after self-consistency was restored; this implies that their fit to the charge density in the core region was fairly poor but that self-consistency screens out small core errors so that they are of no consequence to the important features of the calculation.

We fit the charge density by first placing a charge

$$(A_1\beta_1/\pi r)(\beta_1 r^2-\tfrac{1}{2})e^{-\beta_1 r^2} + (A_2\beta_2/\pi r)(\beta_2 r^2-\tfrac{1}{2})e^{-\beta_2 r^2}$$

on each atom with $A_1\beta_1+A_2\beta_2=0$, $A_1+A_2=29$, $\beta_1=80$ bohr^{-2}, and $\beta_2=20$ bohr^{-2}. This, together with the 29 protons, gives a Coulomb potential

$$V(r)=-(A_1e^{-\beta_1 r^2}+A_2e^{-\beta_2 r^2})/r\ .$$

We then minimized the rms error by varying the coefficients of 31 Gaussians of the form $(\beta/\pi)(\frac{3}{2}-\beta r^2)e^{-\beta r^2}$ and 104 symmetrized combinations of plane waves of the form $\langle e^{i\vec{G}\cdot\vec{r}}\rangle\cos(k_z z)$, where we used symmetrized combinations of the five smallest 2D reciprocal-lattice vectors $\langle e^{i\vec{G}\cdot\vec{r}}\rangle$ and 21 values[8] of $k_z=n(2\pi/5a)$ and excluded $\vec{K}=\vec{G}+\vec{k}_z=0$. These Gaussians contain no net charge and yield a Coulomb potential $e^{-\beta r^2}$. Thus our charge fit automatically yields charge neutrality. We took β's ranging between 40 000 and 0.42 bohr^{-2}. Longer-range Gaussians had too much overlap with the plane waves and caused numerical instabilities in the rms error minimization. We note that SGA had 2% deviations from charge neutrality which they removed with a simple multiplicative factor. To check the accuracy of our fitting procedure we removed the charge-neutrality constraint $A_1+A_2=29$ and obtained a 0.008% deviation from neutrality (i.e., we obtained 203.017 electrons). We fit the exchange-correlation potential with the same 31 Gaussians $e^{-\beta r^2}$ and 105 symmetrized plane-wave combinations including $\vec{K}=0$. In the repeated film configuration the average Coulomb potential is arbitrary.[9] The Coulomb potential obtained from the fit to the charge density reaches a limiting value well before the middle of the region between films. We shift the Coulomb potential by an additive constant to make the limiting value zero. This makes the energy of the highest occupied electron state equal to the negative of the work function.

In order to detect long-range surface states and to better define the energy gaps in the 2D BZ we stretched our 7-layer film to 19 layers (22 layers including selvage region). The stretched film potential for $0<z<a/4$ is taken to be identical to that of the thinner film. We then reflect in the z plane, translate by a lattice vector $a(-\frac{1}{2},0,\frac{1}{2})$, and reflect in the x plane to get

$$(x,y,z)\rightarrow(x,y,-z)\rightarrow(x-\tfrac{1}{2}a,y,-z+\tfrac{1}{2}a)\rightarrow(-x+\tfrac{1}{2}a,y,-z+\tfrac{1}{2})$$

which gives us the potential in the fundamental wedge of the stretched film for $a/4<z<a/2$. The potential in the $0<z<a/2$ region is reflected in the z plane and translated by $(0,0,a)$ to get

$$(x',y',z')\rightarrow(x',y',a-z')$$

which yields the potential for $a/2<z<a$. The potential in the $0<z<a$ region is then successively translated by $(0,0,a)$ to yield the potential for $a<z<3a$. The potential for $3a<z<11a/2$ is taken to be that of thin film (between $0<z<5a/2$). This potential is then fit in the same way as the thinner film except that coefficients of identical Gaussians

on planes 0 through 5 have a common coefficient and 41 rather than 21 values of k_z are used. This smaller number of k_z's relative to the 22/10 ratio of film thicknesses is quite sufficient; the coefficients of the largest k_z terms are more than 4 orders of magnitude smaller than the coefficients of the small k_z terms. This stretching procedure should be considerably more accurate than the usual method[6] of taking matrix elements involving an interior basis function to be identical to the corresponding bulk matrix element even if the other basis function is a surface-plane function.

III. RESULTS

In Fig. 1 the energy bands of the 7-layer film are displayed along the $\bar{\Delta}$, $\bar{Y}$, and $\bar{\Sigma}$ directions of the 2D BZ. The continua and gaps in states of various symmetry at $\bar{\Gamma}$, $\bar{X}$, and $\bar{M}$ are obtained from the 19-layer calculation as are the surface states indicated at these symmetry points. (In a 19-layer film, all surface states and resonances, except those of such long decay length as to be experimentaly undetectable, are easily determined from the decay of the planar projections of the charge density associated with each eigenstate. The arbitrary criterion of requiring some fraction of the charge on the first two planes, which is often applied for thinner films, was not used. This criterion can occasionally cause a thin-film standing-wave resonance which disappears as the film gets thicker to be misinterpreted as a true surface resonance.) Every surface state at these points in the 19-layer film also occurs in the 7-layer film although, as can be seen in the figure, in some cases the degeneracy between pairs on the two faces is split by overlap in the thinner film. At the symmetry points there appears to be[10] a one-to-one correspondence in our and SGA's d-band surface states. In addition at $\bar{\Gamma}$ (at -7.31 eV in Fig. 1) both we and SGA have a strong surface resonance state. At -7.80 and -7.87 eV we have strong $\bar{X}_3$ surface resonances which were not obtained by SGA.[10] We also have an $\bar{X}_3$ surface state at -1.54 eV as well as $\bar{X}_1$ and $\bar{X}_3$ surface states just below E_F which arise from the bulk p-state X_4'; these were not obtained by SGA.

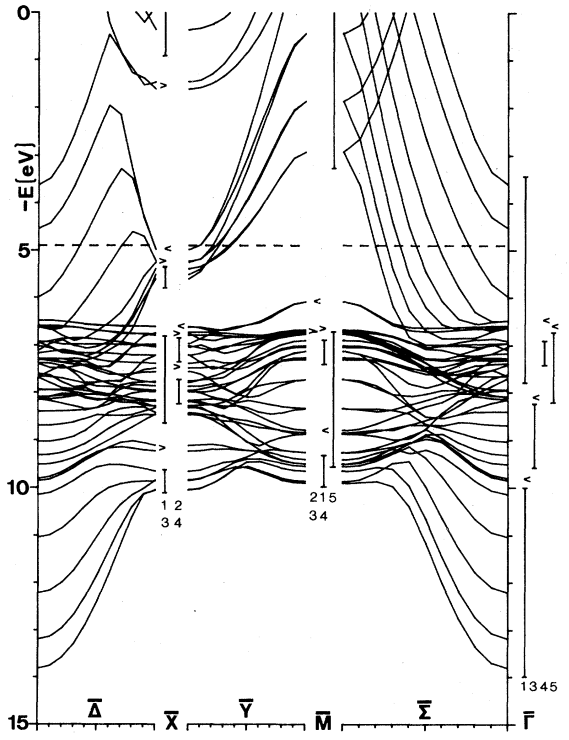

FIG. 1. Energy bands of 7-layer Cu(001) film. The vertical lines represent the bulk continua at $\bar{X}$, $\bar{M}$, and $\bar{\Gamma}$ and are taken from the 19-layer film calculation. The arrowheads represent surface states at those points. When two symmetries have the same bulk continuum, $>(<)$ represents the symmetry with greater (lesser) index.

Our work function is 4.91 eV, whereas SGA obtained 4.5 eV. Very recently, using the linearized augmented-plane-wave method and the Hedin-Lundqvist correlation potential, Wang, Freeman, and Krakauer[11] obtained a work function of 4.94 eV for a 5-layer Cu(100) film. There are experimental values of 4.58, 4.59, 4.76, and 5.10 eV to be found in the literature.[12–15] For Al(111), where experimental values of the work function are consistent, our[16] calculated values are well within 0.1 eV of experiment. Thus in spite of some uncertainty in the effect of the d bands, we have confidence in our ability to calculate work functions accurately. The top of our d bands lies 1.82 eV below the Fermi energy, which may be compared with SGA's 1.5 eV and an experimental value of 2.03 eV. The fact that the calculated d bands lie too high can be attributed to the self-interaction error[17] inherent in the Kohn-Sham approximation.

Figure 2 is a plot of contours of constant charge density in a (100) plane of a 7-layer Cu(001) film. It differs from SGA's plot in two respects. Our outermost contours are noticeably flatter than theirs; this was to be expected because of the extra variational freedom afforded by the floating Gaussians in our basis set. The charge density which we calculate at the octahedral interstitial points is about $\frac{2}{3}$ as large as that we estimate from SGA's contour plot. Our values are[18] (reading from center plane outward) 22.67, 22.88, and 22.17 millielectrons bohr^{-3}. We cannot account for this discrepancy but we note that our values compare well with values obtained from a superposition of atomic change densities (21.50,

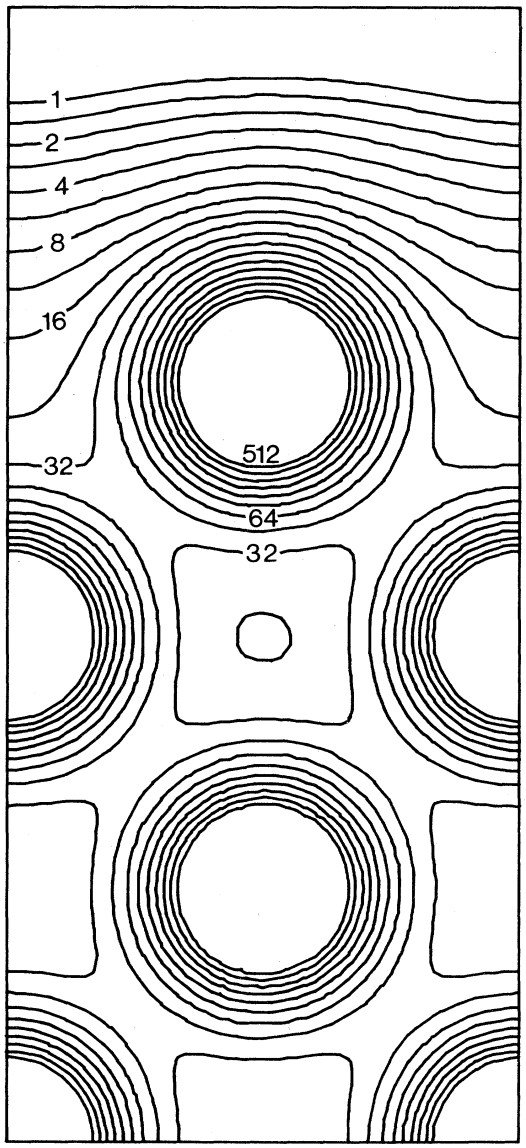

FIG. 2. Contours of constant charge density in units of millielectrons bohr^{-3} for the 7-layer Cu(001) film in the (100) plane. Successive contours are in the ratio of $\sqrt{2}$.

21.50, and 21.48 millielectrons bohr^{-3}). *(Note added:* Smith has informed us that SGA's contours were misnumbered by one increment, e.g., their published contour 16 is really $16/\sqrt{2}$. Thus their interstitial charge densities lie between 19.52 and 27.61 a.u., in agreement with ours.)

Figure 3 is a plot of the 7-layer Cu(001) planar *d* and *sp* DOS obtained from a Löwdin[19] projection. We[20] have recently shown that the Löwdin projection works extremely well even in cases where the Mulliken[21] decomposition breaks down so badly that it yields a negative DOS. Note that not only does the surface *d* DOS have the expected narrowing but the surface *sp* charge,[22] obtained by integrating the DOS up to E_F, is 12% larger than the bulk. This will be discussed further in the next section.

Figure 4 is the 19-layer Cu(001) energy bands of $\bar{\Delta}_2, \bar{Y}_2$, and $\bar{\Sigma}_2$ symmetry and Fig. 5 is the bands of $\bar{\Delta}_1$, $\bar{Y}_1$, and $\bar{\Sigma}_1$ symmetry. The bulk continua and surface states (ss) of all symmetries are indicated at the symmetry points $\bar{\Gamma}$, $\bar{X}$, and $\bar{M}$ in both figures. The atomic orbitals for every symmetry are given in Table II of Ref. 23. There is a $\bar{\Gamma}_4$-$\bar{\Delta}_2$-$\bar{X}_2$ and a $\bar{\Gamma}_5$-$\bar{\Delta}_2$-$\bar{X}_4$ ss band well above the top of the $\bar{\Delta}_2$ bulk bands. The only other $\bar{\Delta}_2$ ss band extends from the $\bar{X}_4$ ss at -7.48 eV only 10% of the way to $\bar{\Gamma}$. The other $\bar{\Gamma}_5$ degenerate partner extends as a broad $\bar{\Delta}_1$ surface resonance bending down in energy until it hits the top of a $\bar{\Delta}$ energy gap and then following the top of the gap upward in energy 80% of the way to $\bar{X}$. This gap, which pinches off and reopens 70% of the way to $\bar{X}$ contains two $\bar{\Delta}_1$ ss bands to the left of the pinch. The upper band continues as a resonance to $\bar{\Gamma}_1$ at -7.27 eV; the lower band continues as a resonance to $\bar{X}_3$ at -7.80 and -7.87 eV. The $\bar{\Gamma}_3$ ss continues as a $\bar{\Delta}_1$ resonance to the top of a narrow gap 20% of the way to $\bar{X}$. The gap contains a $\bar{\Delta}_1$ ss band at -8.32 eV halfway between $\bar{X}$ and $\bar{\Gamma}$. A $\bar{\Delta}_1$ ss band extends all the way from the $\bar{\Gamma}_1$ ss to the $\bar{X}_3$ ss in the lowest $\bar{\Delta}$ gap. There are three nearly-free-electron-like $\bar{\Delta}_1$ ss bands in the high-lying gap. The lower two extend only 10% of the way to $\bar{\Gamma}$; the highest extends 30% of the way. $\bar{Y}_1$ and $\bar{Y}_2$ differ only by an interchange in *A*- and *B*-plane basis functions. Thus both symmetries occur in the nearly-free-electron ss bands emanating from $\bar{X}$. The $\bar{X}_2$ ss continues to $\bar{M}_2$ as a $\bar{Y}_2$ ss band whereas the $\bar{X}_4$ ss continues as the highest $\bar{Y}_1$ *d* band to $\bar{M}_3$. It is a diffuse ss in the 40% of the band near $\bar{X}$ and the 30% near $\bar{M}$ but is not a ss between. The lower $\bar{X}_4$ ss becomes a very broad $\bar{Y}_1$ resonance which narrows and sweeps upward from the middle of the band to connect with the $\bar{M}_3$ ss. The $\bar{X}_3$ resonance at -7.80 and -7.87 eV continues only 10% of the way to $\bar{M}$ as a $\bar{Y}_2$ resonance. The lowest $\bar{X}_3$ ss extends as a $\bar{Y}_2$ ss band in a broad gap halfway to $\bar{M}$; a diffuse $\bar{Y}_1$ ss band extends a short distance at the bottom of this gap. A $\bar{Y}_1$ ss band extends from the $\bar{M}_1$ ss in a narrow gap 60% of the way to $\bar{X}$; a second $\bar{Y}_1$ ss band runs for a short distance in the top of the gap. There are only two $\bar{\Sigma}_2$ ss bands. One running above the top of the *d* bands joins $\bar{\Gamma}_5$ to $\bar{M}_2$ and the other runs from 20% to 60% of the way between $\bar{\Gamma}$ and $\bar{M}$ at the bottom of the large $\bar{\Sigma}_2$ gap. A $\bar{\Sigma}_2$ resonance band of varying strength and width runs all along the top of that gap joining the $\bar{\Gamma}_3$ and $\bar{M}_3$ ss. The $\bar{M}_4$ ss connects to a $\bar{\Sigma}_1$ ss band which continues along the top

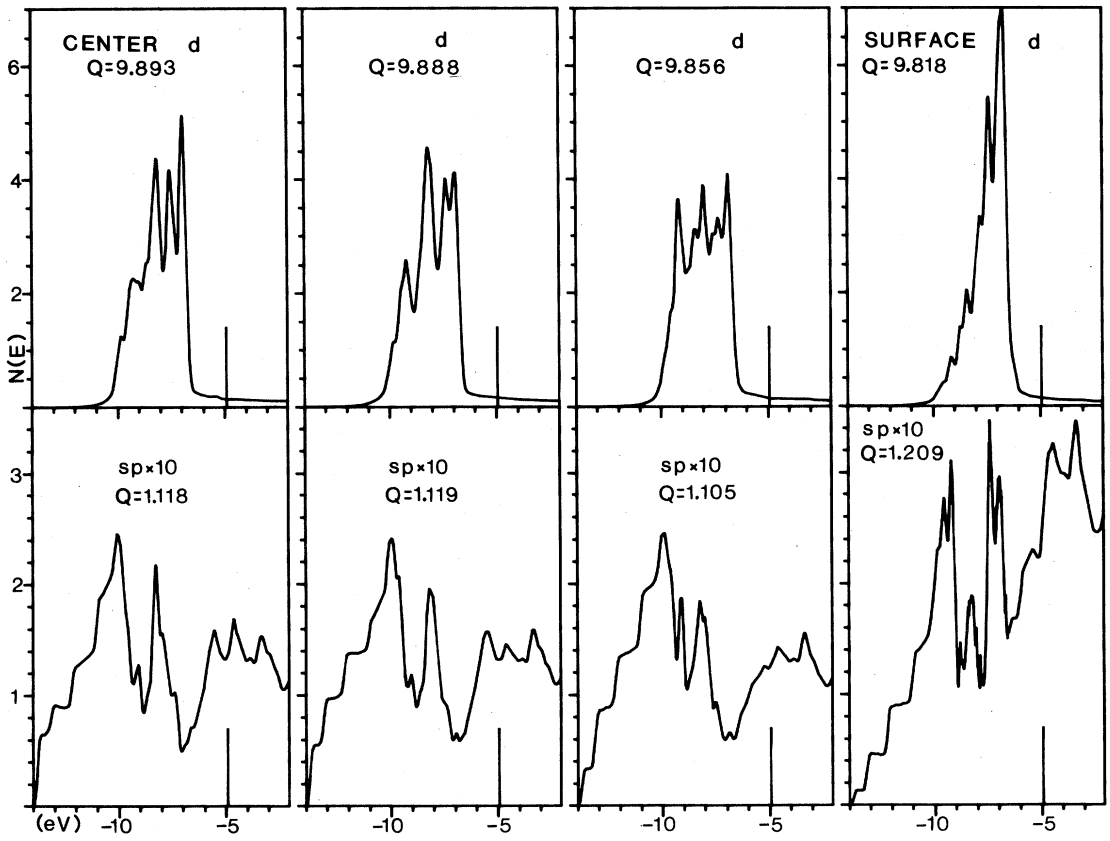

FIG. 3. Planar d and sp densities of states for the 7-layer Cu(001) film in units of electrons per eV. Q is the charge which is obtained by integrating the DOS up to the vertical lines, E_F.

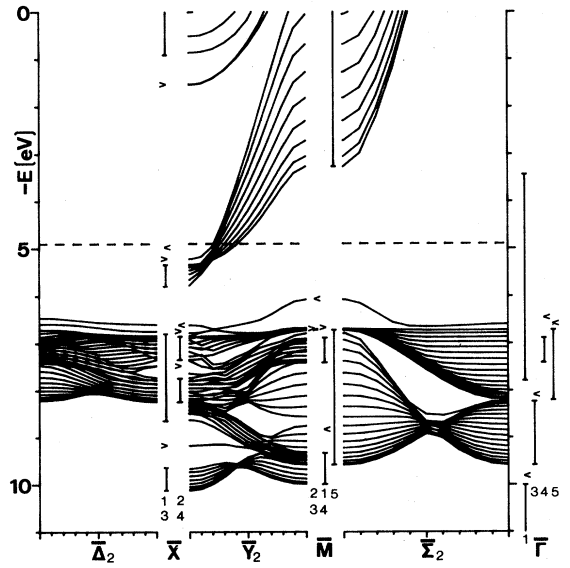

FIG. 4. Energy bands of $\bar{\Delta}_2$, $\bar{Y}_2$, and $\bar{\Sigma}_2$ symmetry for the 19-layer Cu(001) film. The bulk continua and surface states of $\bar{\Gamma}$, $\bar{X}$, and $\bar{M}$ are as in Fig. 1.

of the d bands until the sp bands sweep into the d bands about 35% of the way to $\bar{\Gamma}$; it continues as a strong resonance another 25% of the way to $\bar{\Gamma}$. A small gap opens up just below the resonance and contains a short $\bar{\Sigma}_1$ ss band at about -7.30 eV. A large number of $\bar{\Sigma}_1$ resonances develops out of the $\bar{\Gamma}_4$ and $\bar{\Gamma}_5$ ss and $\bar{\Gamma}_1$ resonance at -7.27 eV and extend 40% of the way to $\bar{M}$. A $\bar{\Gamma}_1$-$\bar{\Sigma}_1$ ss band runs along the bottom of a wide gap about 45% of the way to $\bar{M}$. A broad $\bar{\Sigma}_1$ resonance band emanates from the $\bar{M}_1$ ss and extends halfway to $\bar{\Gamma}$.

IV. DISCUSSION

The most striking feature of these bands is the $\bar{M}_2$ ss which lies 0.66 eV above the top of the $\bar{M}_2$-$\bar{M}_3$ continuum (in agreement with SGA). That continuum is only 0.022 eV wide. This is due to the $\bar{M}_2$ ($\bar{M}_3$) basis functions consisting of d_{xy} orbitals on B (A) planes only. Thus the nearest neighbors which contain basis functions are two planes away and in a direction along which the basis orbitals

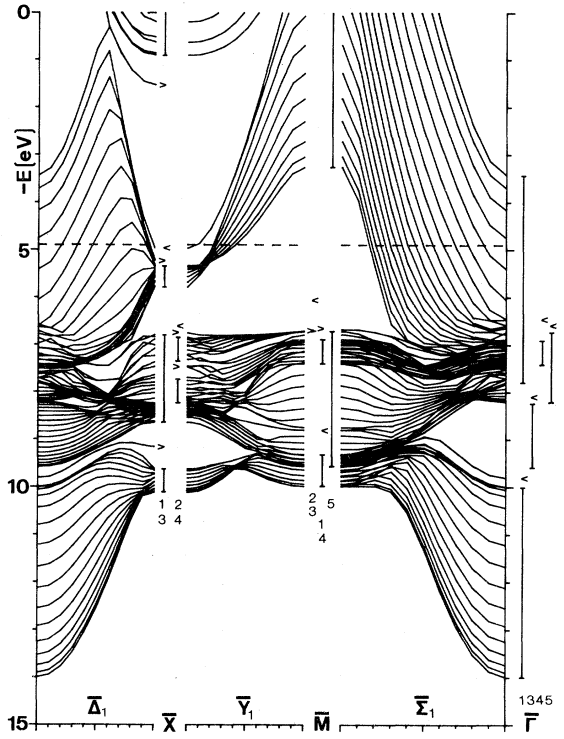

FIG. 5. Energy bands of $\bar{\Delta}_1$, $\bar{Y}_1$, and $\bar{\Sigma}_1$ symmetry for the 19-layer Cu(001) film. The bulk continua and surface states at $\bar{\Gamma}$, $\bar{X}$, and $\bar{M}$ are as in Fig. 1.

have a node. Because the coupling between basis functions is so weak, states are pushed out of the $\bar{M}_2$-$\bar{M}_3$ continuum by an amount equal to the deviation between the potential they see and that seen by bulk basis functions. In Table I are listed the surface energy shifts (relative to the center layer) of the Cu atomic d orbitals which were used to construct the Bloch basis functions. Note $\Delta E_{xy}=0.66$ eV. Although the other ΔE_d are larger, those d orbitals appear in representations that have orbitals on all sites and their ss are not pushed so far out of the bulk continuum.

We should now like to give a brief physical explanation of why the surface potential appears so much less attractive than the bulk potential to d electrons. It is not due to the missing potentials from sites outside the surface. Anderson[24] has shown and we have confirmed with parametrized calculations that, to first order in the overlap, the effect of neighboring-site potentials on diagonal localized-orbital matrix elements is canceled by the orthogonalization of the localized orbital to the orbitals on the neighboring sites. For the sp electrons overlap with neighboring sites is large and the cancellation does not occur; in fact the orthogonalization effects overwhelm the attractive potential and

TABLE I. Difference in energy of atomic d orbitals calculated at surface and center plane sites (in eV).

xy	x^2-y^2	$3z^2$-r^2	yz,xz
0.66	0.82	0.78	0.99

the neighboring sites are effectively repulsive to sp electrons. The effect of missing repulsive neighbors is to induce a large surface excess of sp charge. [Extrapolating from our[1] calculated excess charge[25] for Cu(111), we estimate this sp surface excess to be about 0.35 electrons per atom.] This large excess surface charge is reduced (as is the initially bulklike d surface charge) by its own repulsive Coulomb potential so that the net self-consistent surface excess charge shown in Fig. 3 is only 0.048 electrons per atom. It is this self-consistent repulsive Coulomb potential due to the sp surface excess charge which forces surface states out of the top of the d bands. We can now understand why the effect is stronger in Cu than in Ni. Even though Ni starts out with a much larger surface excess charge (owing to E_F cutting the narrowed surface d DOS), it requires a much weaker repulsive potential to reduce the surface excess charge to a few hundredths of an electron per atom. This is because the DOS at E_F is an order of magnitude larger in Ni than in Cu. We note that Ajmani *et al.*[26] obtain a surface charge deficit for a 5-layer Cu(001) film. This is inconsistent with the repulsive surface potential which they must have to get the d ss which they show. They also find a bulk d population of only 9.2 electrons per atom, compared with our value of 9.89. This we attribute to their use of the Mulliken[21] population analysis which we have shown[20] can yield unphysical results (i.e., negative densities) when long-range s and p orbitals are involved.

ACKNOWLEDGMENT

This work was supported by the National Science Foundation under Grant No. DMR-80-19518.

APPENDIX

Smith *et al.*[4] required 68 iterations to obtain convergence of the planar average of their potential to within 50 meV. We here describe the iterative procedure which enabled us to obtain convergence to within 12 meV after only 24 iterations. A similar scheme, valid only for weak pseudopotentials, has been discussed by Kerker.[27] Usually one takes as the input to the $(n+1)$th iteration

$$V_{n+1}^{\text{in}}=(1-\alpha)V_n^{\text{in}}+\alpha V_n^{\text{out}}=V_n^{\text{in}}+\alpha\Delta_n\ , \qquad \text{(A1)}$$

where $\Delta_n=V_n^{\text{out}}-V_n^{\text{in}}$ and V_n^{out} is the potential ob-

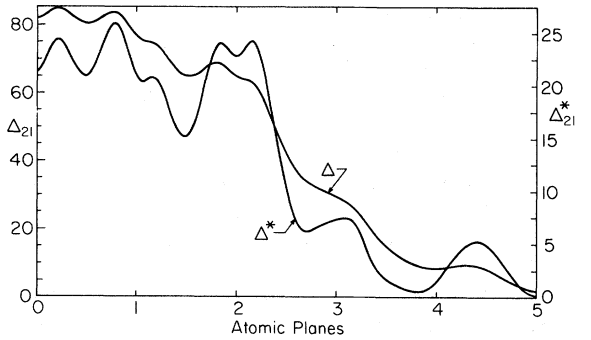

FIG. 6. Planar average of Δ_{21}, the difference between the input and output potentials for the 21st iteration, and of Δ^*_{21} which is obtained from Eq. (A4) in meV.

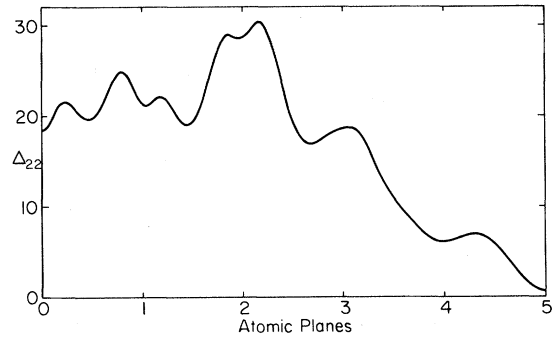

FIG. 7. Planar average of Δ_{22} in meV.

tained from the charge density of the nth iteration. This scheme works well for bulk crystals where the requirement that each unit cell be identical precludes long-range Coulomb contributions to Δ. In a film, however, a small change in input potential can cause a small amount of charge to move a large distance giving a large change in V^{out}. When this V^{out} is fed into the next input potential it results in an even larger change (of opposite sign) in the next V^{out} and convergence in the iterative procedure is not obtained unless α is taken to be very small which causes the convergence of the short-range differences between V^{in} and V^{out} to be interminable.

All our potentials are expanded in Gaussians V_G and plane waves V_K. We make a partial Fourier transformation V_{GK} of V_G with $\vec{K}$ restricted to the set used in V_K. The short-range part of the potential is taken to be $V_G - V_{GK}$ (the sum over all Gaussians and $\vec{K}$'s in the set is implied) and the long- to medium-range part is $V_K + V_{GK}$. We then weight the input and output potentials as in (A1) with an additional weighting proportional to $K^2/(K^2+\lambda^2)$ for V_K and V_{GK}, where λ^2 is a parameter on an equal footing with α, to obtain

$$V^{\text{in}}_{n+1} = (1-\alpha)(V^{\text{in}}_K + V^{\text{in}}_G)_n + \alpha \left[\frac{K^2(V^{\text{out}}_K + V^{\text{out}}_{GK})}{K^2+\lambda^2} + \frac{\lambda^2(V^{\text{in}}_K + V^{\text{in}}_{GK})}{K^2+\lambda^2} + (V^{\text{out}}_G - V^{\text{out}}_{GK}) \right]_n . \tag{A2}$$

After a little rearranging this can be written

$$V^{\text{in}}_{n+1} = V^{\text{in}}_n + \alpha \Delta^*_n , \tag{A3}$$

where

$$\Delta^*_n = \left[\frac{K^2(V^{\text{out}}_K - V^{\text{in}}_K)}{K^2+\lambda^2} - \frac{\lambda^2(V^{\text{out}}_{GK} - V^{\text{in}}_{GK})}{K^2+\lambda^2} + (V^{\text{out}}_G - V^{\text{in}}_G) \right]_n . \tag{A4}$$

In this calculation we used values of α between 0.1 and 0.6 and took $\lambda^2 = \gamma(2\pi/a)^2$ with $\gamma = 0.1$ or 0.4. Occasionally the long-range part of Δ^*_n will begin to break into undamped oscillations (as a function of n). This can be damped out by taking

$$V^{\text{in}}_{n+1} = V^{\text{in}}_n + \alpha \Delta^*_n + \beta \Delta^*_{n-1} . \tag{A5}$$

The efficacy of Δ^* is demonstrated in Figs. 6 and 7. The planar average of Δ and Δ^* (with $\gamma = 0.1$) of iteration 21 are plotted in Fig. 6. From $V^{\text{in}}_{22} = V^{\text{in}}_{21} + 0.15\ \Delta^*_{21}$ the Δ_{22}, whose planar average is plotted in Fig. 7, is obtained. Since the zeroth Fourier transform of the Coulomb potential in our fitting scheme is arbitrary, we have shifted these curves to make them small in the region outside the film. Note that Δ_{21} spans a range of 83 meV whereas Δ_{22} spans only 30 meV. Note further that the relatively weak peak around the second atomic plane in Δ_{21}, although much reduced in absolute magnitude, is by far the most prominent feature in Δ_{22}. It would have been much more prominent if the Δ_{21} to Δ^*_{21} transformation had not strongly emphasized that feature. It is almost as if the Δ to Δ^* transformation anticipates large excursions in the Δ's of future iterations so that they can be worked on before they occur.

*Present address: Bell Laboratories, Murray Hill, NJ 07974.

[1]D. G. Dempsey and L. Kleinman, Phys. Rev. B 16, 5356 (1977), and references therein.

[2]D. G. Dempsey, W. R. Grise, and L. Kleinman, Phys. Rev. B 18, 1270 (1978); 18, 1550 (1978).

[3]J. L. Erskine, Phys. Rev. Lett. 45, 1446 (1980).

[4]J. R. Smith, J. G. Gay, and F. J. Arlinghaus, Phys. Rev. B 21, 2210 (1980).

[5]P. Heimann, J. Hermanson, H. Miosga, and H. Neddermeyer, Phys. Rev. B 20, 3059 (1979).

[6]J. A. Appelbaum and D. R. Hamann, Solid State Commun. 27, 881 (1978).

[7]The addition of these extra surface Gaussians reduced the calculated work function of Al by 0.3 eV (see Ref. 14). We cannot give a quantitative estimate of their importance in Cu because we made no calculations without them.

[8]The thickness of the 7-layer film including selvage region is 10 interplanar spacings or $5a$, where a is the Cu lattice constant, 6.83 bohr.

[9]The plane waves give no contribution to the average potential; thus the value obtained from a particular fit depends on how much charge is carried from the core regions into interstitial regions by plane waves and how much by the Gaussians.

[10]Because SGA do not show the symmetry of their surface states and resonances, it is possible that one of their $\bar{X}$ surface features corresponds to one of our $\bar{X}_3$ resonances rather than to our $\bar{X}_4$ surface state at -7.484 eV.

[11]D. S. Wang, A. J. Freeman, and H. Krakhauer, Phys. Rev. B 26, 1340 (1982).

[12]G. A. Haas and R. E. Thomas, J. Appl. Phys. 48, 86 (1977).

[13]P. O. Gartland, S. Berge, and B. J. Slagsvold, Phys. Rev. Lett. 28, 738 (1972).

[14]G. G. Tibbetts, J. M. Burkstrand, and J. C. Tracy, Phys. Rev. B 15, 3652 (1977).

[15]R. W. Strayer, W. Mackie, and L. W. Swanson, Surf. Sci. 34, 225 (1973).

[16]K. Mednick and L. Kleinman, Phys. Rev. B 22, 5769 (1980); D. M. Bylander, L. Kleinman, and K. Mednick, Phys. Rev. Lett. 48, 1544 (1982).

[17]J. P. Perdew and A. Zunger, Phys. Rev. B 23, 5048 (1981).

[18]Figure 2 was drawn from the fit to the actual charge density. The corresponding values of the fit are 22.67, 22.97, and 22.21 millielectrons bohr^{-3}.

[19]P. O. Löwdin, J. Chem. Phys. 18, 365 (1950).

[20]D. M. Bylander, L. Kleinman, and K. Mednick, Phys. Rev. B 25, 1090 (1982).

[21]R. S. Mulliken, J. Chem. Phys. 23, 1833 (1955).

[22]The surface sp charge contains a contribution of 0.122 electrons per atom from the floating Gaussians.

[23]D. G. Dempsey, L. Kleinman, and E. Caruthers, Phys. Rev. B 12, 2932 (1975). The basis functions given in this reference are with respect to x and y being coordinates of the two-dimensional square lattice. To convert into x, y, and z being cubic coordinates of a fcc lattice rotate by 45° about the z axis. Note that for 7- and 19-layer films, the surface plane is a B plane.

[24]P. W. Anderson, Phys. Rev. 181, 25 (1969).

[25]We refer to the atomic-orbital result in Table I of Ref. 1. When we used Wannier-orbital parameters we obtained a surface charge deficit because we did not take into account the large reduction in kinetic (i.e., orthogonalization) energy of surface (relative to bulk) Wannier functions.

[26]M. Mehta-Ajmani, I. P. Batra, E. E. Lafon, and C. S. Fadley, J. Phys. C 13, 2807 (1980).

[27]G. P. Kerker, Phys. Rev. B 23, 3082 (1981).